

Radiation damage in a-SiO₂ exposed to intense positron pulses

D.B. Cassidy *, A.P. Mills Jr.

Department of Physics and Astronomy, University of California, 3401 Watkins Drive, Riverside, CA 92521-0413, USA

Received 10 April 2007

Available online 24 April 2007

Abstract

In addition to its numerous technological applications amorphous silica (a-SiO₂) is also well suited to the creation and study of exotic atoms such as positronium (Ps) and muonium. In particular, a dense Ps gas may be created by implanting an intense positron pulse into a porous a-SiO₂ sample. However, such positron pulses can constitute a significant dose of radiation, which may damage the sample. We have observed a reduction in the amount of Ps formed in a thin film of porous a-SiO₂ following irradiation by intense positron pulses, indicating the creation of paramagnetic centers. The data show that the primary effect of the irradiation is the inhibition of Ps formation, with no significant change in the subsequent Ps lifetime, from which we deduce that damage centers are created primarily in the bulk material and not on the internal surfaces of the pores, where they would be accessible to the long-lived Ps. We find that the damage is reversible, and that the system may be returned to its original state by heating to 700 K. The implications of these results for experiments with dense Ps in porous materials are discussed.

© 2007 Elsevier B.V. All rights reserved.

PACS: 78.66.Jg; 78.40.Fy; 78.47.–p; 78.70.Bj

Keywords: Positron; Positronium; Radiation

1. Introduction

A scheme to produce a Bose–Einstein condensate (BEC) of Ps was proposed by Platzman and Mills [1] in which an intense burst of positrons incident on a target containing a small cavity would produce a high density of Ps atoms. It was envisaged that these atoms would cool via collisions with the walls of the cavity to the ambient cryogenic temperature and undergo a phase transition to form a BEC, with a critical temperature [2] of around 15 K. This is many orders of magnitude greater than the critical temperature for alkali metals or hydrogen due to the relatively low mass of Ps. However, the critical temperature will only be this high if the positronium density is $> 1 \times 10^{18} \text{ cm}^{-3}$ or so. To produce a Ps BEC in this way would require the implantation of a positron pulse with an areal density of around 10^{13} cm^{-2} , probably at an energy of a few keV

(to penetrate into the cavity region). A pulse of this nature constitutes a considerable radiation dose, which may have consequences for the properties of the sample and thereby affect the formation of a Ps BEC.

The same approach may also be used to perform experiments at lower densities in which Ps atoms interact with each other but do not form a condensate. In this regard the cavities act as substitutes for magneto-optical atom traps [3] and allow for the study of collective effects within the relatively short Ps lifetime. In a previous experiment [4] Ps–Ps interactions were observed which were thought to be a combination of spin exchange quenching and the formation of the di-positronium molecule (Ps₂). Continued experimentation seeks to isolate these processes using a laser resonance for the Ps₂ molecule [5], which, as a purely leptonic diatomic system has some theoretical interest [6]. These experiments involve a much lower radiation dose per pulse than would be required to observe a Ps BEC, but may still lead to a significant accumulated dose during the course of a long experimental run.

* Corresponding author. Tel.: +1 951 827 2919; fax: +1 951 827 4529.
E-mail address: cassidy@physics.ucr.edu (D.B. Cassidy).

It is well-known that exposure to ionizing radiation can lead to damage in silica glasses (and similar materials) [7]. For the present purposes we use the term *radiation damage* to refer to any center in the system created by the positron beam that affects the formation of Ps or its subsequent lifetime. The experimental technique described here cannot easily distinguish between different types of damage, nor can it provide much structural information; the signal is sensitive only to the amount of long-lived Ps present. The most common way to obtain such information is the technique of electron spin resonance (ESR) [8] which is sensitive to paramagnetic centers. While not all damage centers are paramagnetic many of them are and ESR has been extremely successful in characterizing a wide range of damage mechanisms.

Low energy positrons implanted into a-SiO₂ may form Ps quite efficiently; if the a-SiO₂ is porous (that is, an appreciable fraction of the volume consists of empty voids) some of this Ps may diffuse from the bulk material into the voids. In this case the ground state energy difference is converted into kinetic energy, so that if the Ps loses any energy via collisions in the void it cannot then return into the bulk and will therefore be trapped [9]. The lifetime of Ps trapped in this way depends on the pore size and may approach the vacuum lifetime (142 ns) for voids around 100 nm in diameter [10].

The formation of positronium in the bulk is sensitive to the electron density in the region where the positrons are implanted. The presence of “spur” electrons [11], paramagnetic centers, traps or any kind of scavenging electrons can affect the total amount of Ps created [12]. Furthermore, if centers containing unpaired spins are present on the walls of the voids any Ps that diffuses into them will have an increased decay rate [13] due to spin exchange quenching [14]. Since *long lived* Ps is almost entirely formed in the bulk [9] but decays mostly in the voids, such centers would be expected to increase the Ps decay rate but have little effect on the amount of Ps formed. Conversely, damage that exists only in the bulk might be expected to inhibit the formation of Ps, but should hardly affect its subsequent decay rate.

In the work we report here, radiation damage was created in a thin film of a-SiO₂ by irradiation with a pulsed low energy positron beam. The damage was essentially stable at room temperature and entirely annealed out at ~700 K.

2. Experimental procedure

The experiments were performed using a positron accumulator that has been described in detail elsewhere [15]. This device is capable of providing positron pulses with an areal density up to $\sim 5 \times 10^{10} \text{ cm}^{-2}$ about once per minute. The beam density may be controlled by radially expanding the positron plasma in the accumulator prior to release. This is accomplished simply by varying some of the electric fields used for plasma storage [16].

The beam on target is formed into a pulse about 1 ns wide full width at half maximum (FWHM) by an electrostatic buncher [17] that applies a pulsed parabolic potential across the spatial extent of the plasma. In addition to temporal compression, the buncher also accelerates the beam to an (average) energy of 1.5 keV.

The sample used was a ~450 nm thick film of meso-porous silica (MCM-41) grown on a silicon substrate. The pores were ~3 nm in diameter and were interconnected in one dimension only [18]. The porosity was ~60%.

The data were recorded as single-shot lifetime spectra [19] using a 50 mm diameter by 40 mm thick cylindrical PbF₂ Cherenkov radiator, optically coupled to a Hamamatsu H3378–50 photomultiplier tube (PMT). The anode of the PMT was connected directly to a fast oscilloscope with a sampling rate of 20 Giga-samples per second. For the detection of low energy gamma rays, Cherenkov radiators are extremely inefficient compared to most scintillators. However, this type of detector does help mitigate saturation problems and provide the best possible temporal resolution. Using a fast micro channel PMT (for example a Hamamatsu R3809U–50) it is possible to obtain a sub-nanosecond time response, but such tubes typically have small photo-cathodes so that only small PbF₂ crystals may be effectively used, with a concomitant reduction in detection efficiency. The detector used here was a compromise between efficiency and timing and had a response of ~4 ns (FWHM), determined by a combination of the response time of the PMT and the light collection from the large crystal.

The lifetime spectra so obtained were integrated automatically and the “delayed fraction” (f_d) calculated. This is defined as the integrated area of the lifetime spectrum from 20 ns to 150 ns, divided by the total area. This parameter is sensitive to the Ps lifetime as well as the fraction of Ps created per incident positron.

The mean positron implantation depth \bar{z} was estimated to be ~60 nm using the formalism of Algiers and co-workers [20] and an average beam energy of 1.5 keV, a porosity of 60% and a bulk silica density of 2.2 g/cm³. The sample averaged radiation dose per pulse is then

$$D \approx \frac{n_p E_b}{\rho_s A_b \bar{z}} = \rho_b \times 4.5 \times 10^{-8} [\text{Gy}], \quad (1)$$

where n_p is the number of positrons per pulse, E_b is the energy per positron (Joules), ρ_s is the sample density, corrected for the porosity (kg/cm^3), A_b is the cross sectional beam area (cm^2) and ρ_b is the beam areal number density (cm^{-2}). Because of positron diffusion, the beam energy spread and the motion of secondary (spur) electrons we estimate that this is probably accurate to $\sim \pm 25\%$. A more precise determination of the radiation dose per pulse would require a detailed consideration of all pertinent energy loss, scattering and diffusion mechanisms. Nevertheless, for comparative purposes here this approximation is sufficient. We note that we neglect any contribution from

the annihilation radiation since the stopping power for gamma rays in this material is extremely low.

All data were taken after heating the sample to 700 K for an hour or so. This returned f_d to the same level (to within 5%) each time, implying that this process repaired all damage created by previous irradiations.

3. Results and discussion

3.1. Temperature dependence

Fig. 1 shows the accumulation of damage as a function of the radiation dose at various temperatures. These data were taken using a magnetic field at the target of 0.5 T and a beam density of $2 \times 10^9 \text{ cm}^{-2}$ which corresponds to a dose of about 90 Gy/pulse. The top panel (a) is a small section of the 290 K data and is meant to show the size of typical error bars as the rest of the data (b) are plotted as lines for clarity. The horizontal and vertical error bars show the region over which the data has been averaged and the statistical error obtained from the averaging respectively. These data show that the initial rate of damage accumulation is essentially independent of the temperature, except possibly at the highest temperature.

The data shown in Fig. 1(b) have two distinct regions: an initial linear part at low doses followed by another linear region with a much lower slope at higher doses. This piecewise linearity is very similar to observations made by Galeener and co-workers [21] who studied the creation of ESR signals in vitreous silica following X-ray bombardment (although the signal was ascribed to electrons released by the X-rays [22]). They attributed the initial fast component to a process wherein pre-existing defect sites were activated by charge transfer and the slower process

to the creation of new defects. Since there are a finite number of pre-existing pre-cursor sites this component saturates, leading to the observed form of the damage accumulation.

This model is quite consistent with the data we present here and following Galeener et al. the data shown in Fig. 1 (b) has been fitted to a function of the form

$$f_d(D) = f_0 - N_0(1 - \exp(-D/D_0)) - R_c D. \quad (2)$$

Here f_0 is an (arbitrary) offset, N_0 represents the total number of pre-existing defects, D is the radiation dose, D_0 is the dose for which the number of pre-existing defects remaining is N_0/e and R_c represents the (constant) rate at which new defects are created. It is of course possible that there are really two activation sites, with one saturating very slowly. Indeed, the data can be fitted to a double exponential function just as well as to Eq. (2). However, for all practical purposes we may simply treat the slow component as linearly increasing with the dose in the manner indicated by Eq. (2).

Fig. 2 shows the values of N_0 and R_c obtained from fitting Eq. (2) to the data of Fig. 1(b). Also shown is R_{ai} which is the *initial* rate at which damage is activated and is the instantaneous slope at the very beginning of the irradiation. That is

$$R_{ai} = \left[\frac{df_d(D)}{dD} \right]_{D=0} = N_0/D_0 \quad (3)$$

It should be remembered that these data are all derived from f_d whose value is essentially arbitrary. That is, the rates shown indicate the change in f_d as a function of the actual dose. While it is possible in principle to convert this

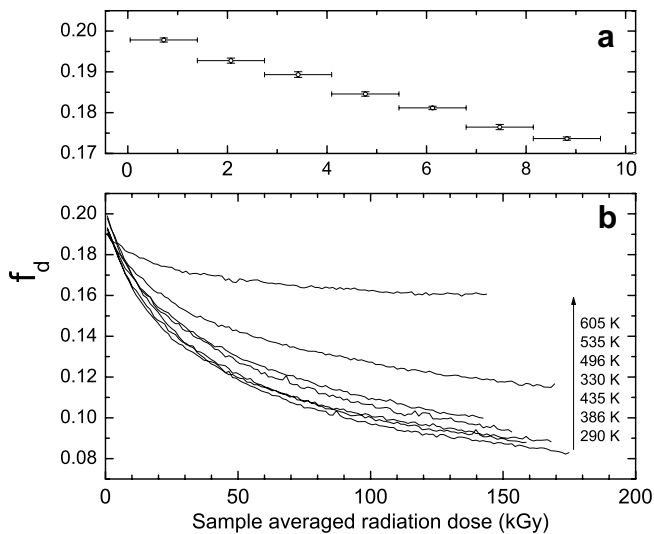


Fig. 1. The damage induced as a function of the radiation dose. The top panel (a) shows the initial damage accumulation at 290 K. The bottom panel shows damage accumulation for a range of temperatures. The legend indicates the temperatures for ascending curves, as indicated by the arrow.

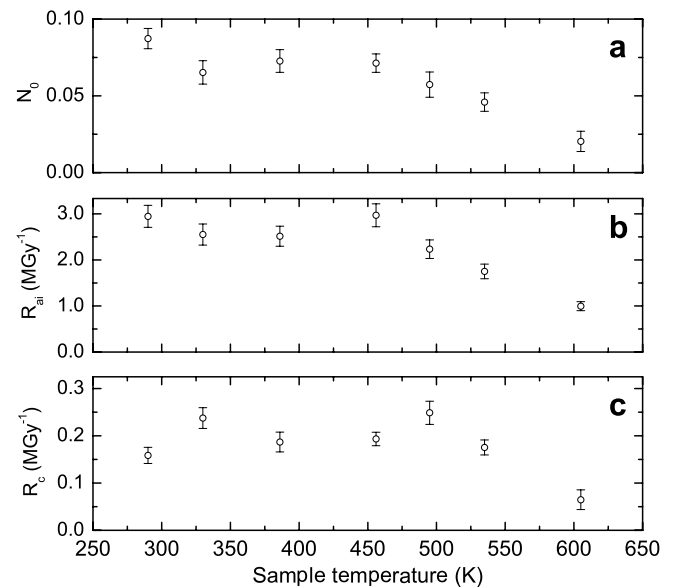


Fig. 2. Parameters obtained from a least squares fit of Eq. (2) to the data in Fig. 1(b). A measure of the number of pre-existing defect sites is given by the parameter N_0 (a). Also shown are the initial rate of damage activation R_{ai} (b) and creation R_c (c). The errors are derived from the fitting procedure and have been increased by a factor of ~ 5 to account for systematic variations between runs.

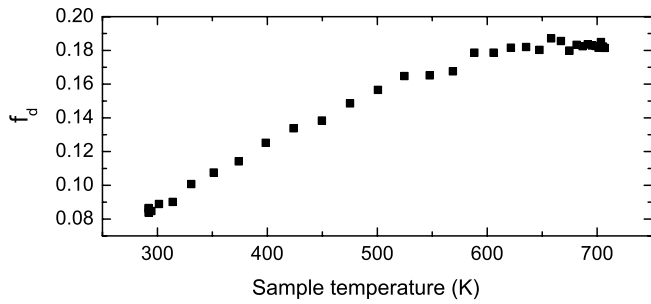


Fig. 3. Almost all damage created by irradiation at room temperature is quickly repaired by heating the sample to 700 K. Each data point is a single-shot and the dump rate was 1 per minute.

number to the total defect number or concentration one would have to make a number of assumptions regarding the details of the (unknown) processes. For the present purposes it is sufficient simply to compare the changes in f_d .

Fig. 1(b) shows that after about 30 kGy or so the amount of damage present is reduced as the temperature is increased. Because of variations in the initial amount of damage present the 330 K curve appears to be out of sequence. However, this offset is accounted for in the fit so that the parameters shown in Fig. 2 are unaffected by it.

Figs. 1 and 2 both show that at low temperatures there is very little variation in the amount of damage created. The effective number of activation sites (N_0) shown in Fig. 2(a) is largely unchanged until around 450 K as is the initial activation rate $R_{a,i}$ shown in Fig. 2(b). The damage creation rate R_c shown in Fig. 2(c) is fairly constant until the temperature exceeds 500 K, where it too begins to fall off. The creation rate is around an order of magnitude less than the (initial) activation rate. This is consistent with the idea that there is a separate (creation) process that requires more energy and is thus slower than the activation process.

The recovery of the system after raising the temperature is quite rapid, as shown in Fig. 3. These data show the effect of heating following irradiation at room temperature. At temperatures above 700 K most of the damage created by irradiation is repaired, with an additional $\sim 5\%$ growth that occurs over a time scale of many hours. When the sample is kept at room temperature following irradiation no change in f_d was observed after 24 h. That is, the damage is stable at room temperature.

3.2. Density dependence

The data shown so far were all taken with the same beam areal density ($2 \times 10^9 \text{ cm}^{-2}$) which corresponds to a sample averaged dose of around 90 Gy/pulse. In order to gain some insight into the effects one might expect using more intense pulses, such as those envisioned for Ps BEC experiments, the accumulation of damage was studied using different beam densities (at room temperature).

The beam density can be varied by allowing the positron plasma to expand in the accumulator prior to release or by changing the magnetic field at the sample. In the latter case

the amount of mixing of the Ps $m = 0$ magnetic sub states [23], and hence f_d , will be different when the field is changed.

Fig. 4 shows damage accumulation for two different densities as obtained by expanding the plasma. The lower density beam creates less damage per pulse, as we would expect and eventually approaches the same saturation level as the higher density beam; the amount of damage present depends only on the radiation dose and not on the dose rate.

The situation appears to be slightly different when a higher magnetic field is used, as shown in Fig. 5. Here the beam density (and the dose per pulse) is about 10 times higher and there is a difference between the high and low density beams. Even at low doses similar to that applied in Fig. 4 the higher density beam seems to create more damage than the lower density beam for a given dose. However, the reduction in f_d in this case is slightly misleading because at these beam densities there is significant spin exchange quenching due to collisions between oppositely polarized triplet Ps atoms [4].

As damage accumulates the amount of Ps formed (and hence the Ps density) decreases, which reduces the amount of spin exchange quenching and thus the high and low

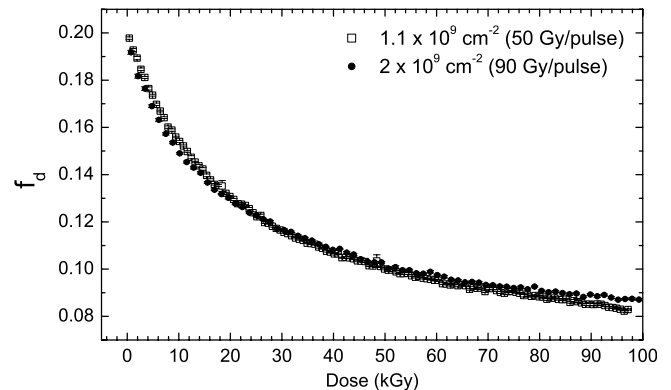


Fig. 4. The accumulation of damage with a low magnetic field (0.15 T) for two different density beams. When scaled for the total dose the amount of damage is essentially independent of the beam density.

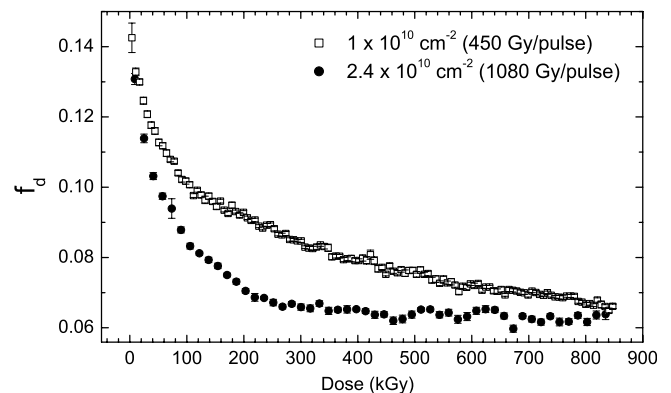


Fig. 5. The accumulation of damage with a high magnetic field (2 T) for two different density beams. The initial value of f_d is less than in previous figures due to magnetic quenching.

density data in Fig. 5 eventually converge. (We note that the higher density data are somewhat distorted as f_d approaches 0.06 which is very close to the Ps detection limit of the system.) This seems to imply that the actual amount of damage created is still proportional to the applied dose.

Even when the beam density is sufficiently high to allow for Ps–Ps interactions it is unlikely that there would be multi-positron interactions occurring in a single pulse. Thus, the damage creation mechanisms are almost certainly single positron effects. However, it is possible in principle for spur electrons from different positrons to interact with each other. In the present case this is unlikely since the smallest mean positron separation is ~ 100 nm, while the spur size is considerably smaller than this (20–60 nm) [24]. For a much higher density beam this would no longer be true and there could very well be additional multi-particle based damage creation (or repair) mechanisms, so that the dose rate might then become important. So far we have observed no indication of this. If a single pulse of density $5 \times 10^{12} \text{ cm}^{-2}$ were used (equivalent to a dose of ~ 225 kGy) then we might expect that the amount of Ps produced as a result would be reduced by a factor of 2 or so due to damage. While this is far from ideal it does not render experimentation to make a Ps BEC in porous silica unfeasible.

The sample was mounted on a manipulator with a computer controlled stepper motor and could be positioned along one axis perpendicular to the beam to within an accuracy of $\sim 25 \mu\text{m}$. Following irradiation with a high density beam (see Fig. 5) approximately $250 \mu\text{m}$ (FWHM) the sample was scanned laterally using a probe beam $\sim 180 \mu\text{m}$ (FWHM) in order to determine the spatial distribution of the damage. To avoid creating additional damage with the probe beam each point measured consisted of only five shots. The measured quantity was f_d versus position, but as is evident from Fig. 5, the damage is created non-linearly. The true beam profile was recovered by converting f_d into an approximate equivalent dose. This was done using an average of the data shown in Fig. 5 to partially account for the density dependent quenching effect. If the damage were entirely localized to the incident beam profile we should expect the data of Fig. 6 to approximate a Gaussian

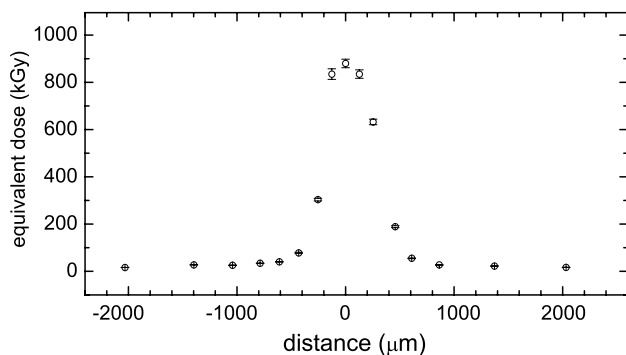


Fig. 6. The damage as a function of position. Zero distance corresponds to the sample position during the prior irradiation. The damage has been inferred from measured values of f_d as described in the text.

profile with a FWHM close to a convolution of the irradiation and probe beams (i.e. $\sim 310 \mu\text{m}$). The observed profile appears to be slightly wider than this ($\sim 400 \mu\text{m}$) which is probably due to saturation, as well as the approximation used to determine the dose.

4. Conclusion

Because the Ps signal is indiscriminate we cannot say what kind of damage has been created in these experiments. In order to determine specific information about the damage sites created it would be necessary to perform supplementary measurements, such as ESR. In fact this has been done before by other researchers, but the results are not as clear as one might hope. Hasagawa and co-workers [25] used both positron annihilation lifetime spectroscopy (PALS) and ESR to study radiation damage in silica glass. Two distinct types of defect were observed using positrons, but these researchers were not able to make a direct correlation between their ESR and PALS data. One possible reason for this is simply that PALS is sensitive to both paramagnetic and diamagnetic defects, while ESR is sensitive only to paramagnetic centers. Hasagawa et al. speculated that E' centers, non-bridging oxygen hole centers and peroxy radicals [26] were likely candidates for the centers they observed.

Fujinami and Chilton [27] have also performed simultaneous positron annihilation spectroscopy and ESR measurements, using silica bombarded with ions. They found centers that trapped positrons that were not observed by ESR and attributed this to dissolved oxygen or charged Frenkel defects. However, since their sample did not return to the un-irradiated state until heated to temperatures above 900 K, it is unlikely we have observed the same type of center here. Fujinami and Chilton [27] point out that there are number of possible charged defects that may trap positrons but be undetectable to ESR. Also, an intriguing possibility [28] is that we may be observing electrons and holes trapped pair wise (negative U trapping [29]) which would be undetectable via ESR, although this is purely speculative.

There are also many well-known paramagnetic centers that are unstable at room temperature (for example, self trapped holes are not stable above ~ 200 K [30]) and future experiments at cryogenic temperatures will be required to ascertain the extent to which these additional defects might impact a Ps BEC experiment, which must necessarily be performed at low temperature.

To summarize, we have observed damage of an unknown nature in a porous a-SiO₂ film created by slow positrons. The dose required to create significant damage is higher than was applied in previous experiments [4] where this effect was negligible. However, it may become important in work using more intense positron pulses. It appears that the amount of damage depends only on the dose, although we cannot rule out additional processes at much higher beam densities. We also do not know if the

damage would prevent Ps formation in the same pulse in which it was itself created. This is important because we have shown that the damage is almost entirely localized to the irradiated area, so that in an experiment with very high densities one could simply move the sample by a 1000 microns or so between shots and avoid the damaged regions. An inspection of the Ps lifetime spectra shows that only the Ps intensity is affected, which is consistent with the idea that the damage is all confined to the bulk. We have found that the damage is stable at room temperature but is completely repaired by heating the sample to 700 K. For non-cryogenic experiments this type damage can be avoided altogether by keeping the sample hot.

Acknowledgements

We are grateful to D.L. Griscom for helpful comments and advice. We acknowledge H.W.K. Tanaka, T. Maruo and N. Nishiyama for providing the silica sample. This work was supported in part by the NSF under Grants DMR 0216927 and PHY 0140382.

References

- [1] P.M. Platzman, A.P. Mills Jr., *Phys. Rev. B* 49 (1994).
- [2] For an excellent review of the properties of Bose–Einstein condensates see A.J. Leggett, *Rev. Mod. Phys.* 73 (2001) 307.
- [3] Standard magneto-optical traps which have been spectacularly successful for the study of ultra-cold atoms (including the formation and manipulation of BEC's) are impractical for Ps because they rely on a copious source of particles (for evaporative cooling) and because the atomic transitions that would be required for Ps would perturb the system to a much larger degree. For a recent review see J. Fortágh, C. Zimmermann, *Rev. Mod. Phys.* 79 (2007) 235.
- [4] D.B. Cassidy, S.H.M. Deng, R.G. Greaves, T. Maruo, N. Nishiyama, J.B. Snyder, H.K.M. Tanaka, A.P. Mills Jr., *Phys. Rev. Lett.* 95 (2005) 195006.
- [5] A.P. Mills Jr., *Rad. Phys. and Chem* 76 (2007); K. Varga, J. Usukura, Y. Suzuki, *Phys. Rev. Lett.* 80 (1998) 1876.
- [6] For example D.M. Schrader, *Phys. Rev. Lett.* 92 (2004) 043401; S. Bubin, L. Adamowicz, *Phys. Rev. A* 74 (2006) 052502.
- [7] G. Pacchioni, L. Skuja, D.L. Griscom (Eds.), *Defects in SiO₂ and Related Dielectrics: Science and Technology*, Kluwer Academic Publishers, Dordrecht, 2000.
- [8] D.L. Griscom, in: D.R. Uhlmann, N.J. Kreidl (Eds.), *Glass: Science and Technology*, Vol. 4B, Academic, Boston, 1990, p. 151.
- [9] Y. Nagashima, Y. Morinaka, T. Kurihara, Y. Nagai, T. Hyodo, T. Shidara, K. Nakahara, *Phys. Rev. B* 58 (1998) 12676.
- [10] See, e.g. D.W. Gidley, K.G. Lynn, M.P. Petkov, J.N. Sun, M.H. Weber, A.F. Yee, in: D.M. Surko, F.A. Gianturco (Eds.), *New Directions in Antimatter Chemistry and Physics*, Kluwer, Dordrecht, 2001, p. 151.
- [11] M. Eldrup, V.P. Shantarovich, O.E. Mogensen, *Chem. Phys.* 11 (1975) 129.
- [12] See for example Y. Kobayashi, K. Ito, T. Oka, K. Hirata, *Rad. Phys. Chem.* 76 (2007) 224.
- [13] D.B. Cassidy, K.T. Yokoyama, S.H.M. Deng, D.L. Griscom, H. Miyadera, H.W.K. Tom, C.M. Varma, A.P. Mills Jr., *Phys. Rev. B* 75 (2007) 085415.
- [14] M. Deutsch, *Phys. Rev.* 82 (1951) 455; R.A. Ferrell, *Phys. Rev.* 110 (1958) 1355; N. Shinohara, N. Suzuki, T. Chang, T. Hyodo, *Phys. Rev. A* 64 (2001) 042702.
- [15] D.B. Cassidy, S.H.M. Deng, R.G. Greaves, A.P. Mills Jr., *Rev. Sci. Instr.* 77 (2006) 073106.
- [16] F. Anderegg, E.M. Hollmann, C.F. Driscoll, *Phys. Rev. Lett.* 81 (1998) 4875; R.G. Greaves, C.M. Surko, *Phys. Rev. Lett.* 85 (2000) 1883.
- [17] A.P. Mills Jr., *Appl. Phys. (Berlin)* 22 (1980) 273.
- [18] For further details regarding the sample and the relevant fabrication methods see S. Tanaka, N. Nishiyama, Y. Oku, Y. Egashira, K. Ueyama, *J. Am. Chem. Soc.* 126 (2004) 4854.
- [19] D.B. Cassidy, S.H.M. Deng, H.K.M. Tanaka, A.P. Mills Jr., *Appl. Phys. Lett.* 88 (2006) 194105.
- [20] J. Algers, P. Sperr, W. Egger, G. Kögel, F.H.J. Maurer, *Phys. Rev. B* 67 (2003) 125404; See also A.P. Mills, R.J. Wilson, *Phys. Rev. A* 26 (1982) 490.
- [21] F.L. Galeener, D.B. Kerwin, A.J. Miller, J.C. Mikkelsen Jr., *Solid State Commun.* 82 (1992) 271; F.L. Galeener, D.B. Kerwin, A.J. Miller, J.C. Mikkelsen Jr., *Phys. Rev. B* 47 (1993) 7760.
- [22] D.B. Kerwin, F.L. Galeener, *Appl. Phys. Lett.* 59 (1991) 2959.
- [23] For example A. Rich, *Rev. Mod. Phys.* 53 (1981) 127.
- [24] L. Xie, G.B. DeMaggio, W.E. Frieze, J. DeVries, D.W. Gidley, H.A. Hristov, A.F. Yee, *Phys. Rev. Lett.* 74 (1995) 4947.
- [25] M. Hasagawa, M. Tabata, M. Fujinami, Y. Ito, H. Sunaga, S. Okada, S. Yamaguchi, *Nucl. Instr. and Meth. B* 116 (1996) 347.
- [26] For example T.E. Tsai, D.L. Griscom, *Phys. Rev. Lett.* 67 (1991) 2517.
- [27] M. Fujinami, N.B. Chilton, *Appl. Phys. Lett.* 62 (1993) 1131.
- [28] This was first suggested to us by D.L. Griscom in a private communication.
- [29] P.W. Anderson, *Phys. Rev. Lett.* 34 (1975) 953.
- [30] D.L. Griscom, *J. Non-Cryst. Solids* 149 (1992) 137; D.L. Griscom, *Phys. Rev. B* 40 (1989) 4224.